Dual-Mode Behavior in Doping-Undoping of Polypyrrole with Alkanesulfonate

Takeo Shimidzu,* Akira Ohtani, and Kenichi Honda
Division of Molecular Engineering, Graduate School of Engineering, Kyoto University, Sakyo-ku, Kyoto 606

(Received February 15, 1988)

Polypyrrole (PPy) films incorporated with a series of 1-alkanesulfonates, $R_nSO_3^-$ ($C_nH_{2n+1}SO_3^-$, n=3—10), were prepared by the electrochemical polymerization of pyrrole in H_2O containing sodium salt of $R_nSO_3^-$. The mass transfer in the PPy matrix of the $R_nSO_3^-$ incorporated PPy (PPy/$R_nSO_3^-$) films were investigated by electrochemical measurements. The electrochemical properties of PPy/$R_nSO_3^-$ were affected by the chain length of the incorporated $R_nSO_3^-$. The incorporation and release of cationic species into the PPy/$R_nSO_3^-$ matrix during an electrochemical oxidation-reduction of PPy were observed and the contribution of cationic species during the doping-undoping process was increased with the dopant size. The PPy/$R_nSO_3^-$ showed a dual-mode behavior during the electrochemical doping-undoping process.

Conducting PPy[1-6] has applications in such equipment as, electronic devices,[7,8] electrochromic displays,[9-11] polymer batteries,[12-15] polymer modified electrodes,[16] functional membranes,[17,18] etc. In these applications, the oxidation-reduction capability accompanying the incorporation-release of ions, which is called "doping-undoping," is an important feature of PPy.[19] Though PPy has been studied most widely, it has not provided any advantageous properties from a practical point of view. Many hybridization procedures of PPy with various functional molecules have been developed so as to improve the properties of PPy.[20-31] Especially, a hybridization procedure utilizing an anodic doping process during the electrochemical polymerization of pyrrole has been actively studied, and many kinds of PPy/functional anion composites were prepared. However, there is a question whether PPy/functional anion composites show stable properties under all redox states of PPy, because incorporated anions (dopants) are usually released from the PPy matrix when PPy is reduced. We reported that the size of the dopant affected the doping-undoping capability of PPy.[32] In recent years, studies of mass transfer in the PPy matrix on the oxidation-reduction of PPy have been reported.[33-36] Either anion releasing or cation incorporating was observed when PPy was electrochemically reduced. In this study, a series of 1-alkanesulfonates was chosen as the dopant[37] and the detailed electrochemical property of PPy/$R_nSO_3^-$ during the electrochemical oxidation-reduction process is discussed.

Experimental

Materials. Pyrrole (Aldrich Chemical Co.) was distilled and stored under an N_2 atmosphere. Potassium chloride (Wako Chemical Co.) and sodium 1-alkanesulfonates, such as sodium 1-propanesulfonate, 1-butanesulfonate, 1-pentanesulfonate, 1-hexanesulfonate, 1-heptanesulfonate, 1-octanesulfonate, 1-nonanesulfonate, and 1-decanesulfonate (Nakarai Chemicals), were used without further purification.

Preparation of PPy. PPy/$R_nSO_3^-$ films on an indium-tin oxide (ITO) electrode (7 cm^2) for elemental analyses, measurements of conductivity, and deionization experiments were prepared by the electrochemical polymerization of pyrrole (0.1 mol dm^{-3}) in H_2O containing sodium salt of $R_nSO_3^-$ (0.1 mol dm^{-3}) under 10 mA galvanostatic electrolysis for 1 h. The thicknesses of these films were estimated by an optical microscopic photograph of the cross section of the PPy/$R_nSO_3^-$. PPy/$R_nSO_3^-$ films on a Pt electrode (0.047 cm^2) for cyclic voltammetry were prepared by an electrochemical polymerization of pyrrole (0.1 mol dm^{-3}) in H_2O containing sodium salt of $R_nSO_3^-$ under potentiostatic electrolysis (1.0 V vs. SCE) for 4.9 mC. A chloride anion incorporated PPy (PPy/Cl^-) on an ITO electrode (7 cm^2) was prepared by the electrochemical polymerization of pyrrole (0.2 mol dm^{-3}) in 0.5 mol dm^{-3} KCl aqueous solution under 10 mA galvanostatic electrolysis for 1 h. The reduced PPy/Cl^- (PPy/Cl^-(red.)) for deionization experiments was prepared by a −2.0 mA galvanostatic electrolysis of the PPy/Cl^- anode in a 0.1 mol dm^{-3} KCl aqueous solution until the potential reached −1.0 V vs. SCE, at which point the incorporated Cl^- was quantitatively released.

Electrochemical Measurements. Cyclic voltammetries were carried out in H_2O containing a 0.1 mol dm^{-3} sodium salt of $R_nSO_3^-$ or KCl. Deionization experiments were carried out by potentiostatic electrolysis of the PPy/Cl^- (red.) anode and the PPy/$R_nSO_3^-$ cathode. The concentration of K^+ in a KCl aqueous solution was measured by an atomic absorption analysis (Shimadzu AA-670). All electrochemical experiments were carried out at room temperature under an N_2 atmosphere using a potentiogalvanostat (Nikko Keisoku NPGS- 301), a function generator (Nikko Keisoku NFG-3), and a coulomb/ampere-hour meter (Hokuto Denko Ltd. HF-201).

Results and Discussion

Electrochemical Properties of PPy/$R_nSO_3^-$. The dopant ratio and conductivity are indicative characteristics for the electrochemical properties of conducting polymers. Table 1 shows elementary analyses and film thickness of the PPy/$R_nSO_3^-$. The S/N ratio, which allowed us to estimate the ratio of incorporated anions to the pyrrole moiety (dopant ratio), increased with the dopant size. The resulting film thickness also increased with the dopant size. Figure 1 shows the conductivity of the PPy/$R_nSO_3^-$ films. The conduc-

Table 1. Elemental Analysis and Film Thickness of $PPy/R_nRO_3^-$ [a)]

Carbon number of dopant	Elemental analysis				Mole ratio S/N	Film thickness /μm
	C	H	N	S		
3	57.3	4.46	14.3	5.54	0.169	18
4	57.3	4.78	13.6	6.23	0.200	23
5	58.4	5.34	12.8	7.45	0.254	24
6	58.9	5.79	11.9	7.99	0.293	25
7	60.0	6.28	11.0	7.84	0.311	25
8	60.6	6.41	10.5	7.64	0.317	26
9	61.1	6.89	9.86	7.46	0.330	27
10	62.0	7.28	9.07	7.26	0.349	33

a) $PPy/R_nSO_3^-$ films were prepared by electrochemical polymerization for 4.7 $C\,cm^{-2}$.

Table 2. Peak Potentials[a)] of $PPy/R_nSO_3^-$ Electrodes

Carbon number of dopant	E_{Pa}	E_{Pc} /mV vs. SEC	$E_{1/2}$
3	−440	−600	−520
4	−450	−600	−525
5	−460	−610	−535
6	−475	−610	−543
7	−480	−720	−600
8	−520	−750	−635
9	−520	−765	−643
10	−510	−670	−590

a) Sweep rate was 50 $mV\,s^{-1}$.

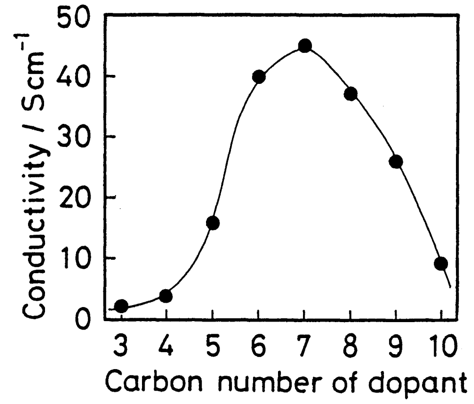

Fig. 1. Relationship between conductivity and carbon number of dopant for $PPy/R_nSO_3^-$.

tivity of the $PPy/R_nSO_3^-$ first increased with the dopant size (n=3—7) and then decreased (n=7—10). In general, the conductivity of the conducting polymer increases with the dopant ratio. However, the optimum conductivity was observed with $PPy/R_7SO_3^-$. The decrease of the conductivity was explained by the decrease of the electron carrier density, which was governed by the alkyl-chain length of the incorporated anion.

Cyclic voltammetry is one of the most important measurement techniques for investigating the electrochemical properties of PPy. Figure 2 shows typical cyclic voltammograms (sweep rates were 20—500 mV s^{-1}) of $PPy/R_nSO_3^-$ (n=3, 5, and 10) in H_2O containing the incorporated anion (0.1 $mol\,dm^{-3}$) as a supporting electrolyte. These cyclic voltammograms reflect the doping-undoping behavior of the incorporated anion, not involving any exchange reactions of incorporated anions (as stated below). Table 2 shows the redox potentials of $PPy/R_nSO_3^-$ at a sweep rate of 50 mV s^{-1}. The redox potentials of $PPy/R_nSO_3^-$ appeared in the range −520—−643 mV, and decreased with the dopant size. It has already been reported that the redox potential is affected by the properties of the incorporated anion.[33)]

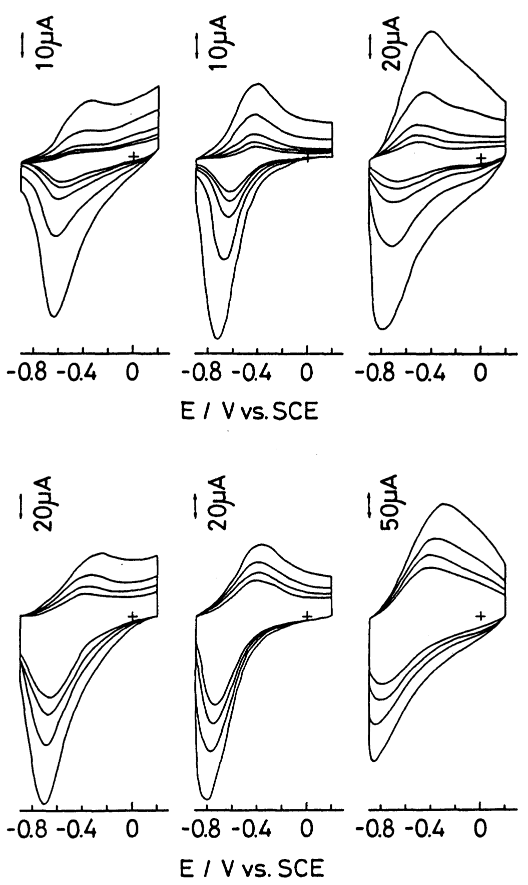

Fig. 2. Cyclic voltammograms of $PPy/R_3SO_3^-$ (left), $PPy/R_5SO_3^-$ (middle), and $PPy/R_{10}SO_3^-$ (right) in H_2O containing the incorporated anion (0.1 $mol\,dm^{-3}$) as a supporting electrolyte. Sweep rate was 20—100 $mV\,s^{-1}$ (upper) and 200—500 $mV\,s^{-1}$ (bottom).

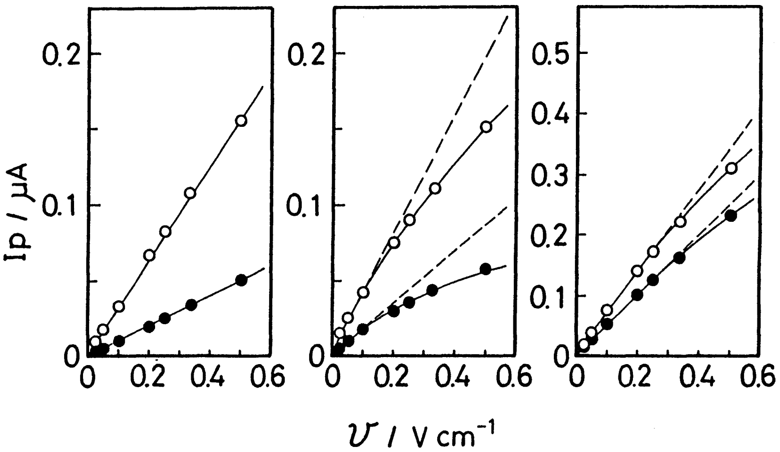

Fig. 3. Relationship between i_p and v for the cyclic voltammograms of PPy/$R_3SO_3^-$ (left), PPy/$R_5SO_3^-$ (middle), and PPy/$R_{10}SO_3^-$ (right). (●); anodic peak current, (○); cathodic peak current.

It is well-known that the relationship between the peak current (i_p) and the sweep rate (v) in a cyclic voltammogram shows the characteristics of mass transfer in the electroactive film on the electrode. The power number (X), the slope of the linear relationship between $\log(i_p)$ and $\log(v)$, is a convenient factor for estimating the mobility of the ionic species in the matrix. In general, X=1 shows that the mobility of the ionic species is higher than the electron-transfer rate, which is called "a surface wave;" X=0.5 shows that the mobility of the ionic species is lower than the electron-transfer rate, "a diffusion-controlled wave." In fact, X can have values from 0.5 to 1.0. Therefore, the contribution of the diffusion-controlled wave behavior is estimated by the X-value. It has been reported that the charge propagation mechanism, surface wave behavior or diffusion-controlled wave behavior, is affected by the properties of the counter ions in a polymer-modified electrode.[38] Figure 3 shows typical i_p-v relationships obtained from Fig. 2. In a surface wave (X=1) i_p is proportional to v, and in a diffusion-controlled wave (X=0.5) i_p is proportional to $v^{1/2}$. At $v<100$ mV s^{-1} all PPy/$R_nSO_3^-$ showed the surface-wave behavior, as in some previous studies on ordinary PPy. However, at $v>100$ mV s^{-1}, PPy/$R_3SO_3^-$ (small-size dopant) and PPy/$R_{10}SO_3^-$ (large-size dopant) showed almost the surface-wave behavior, and PPy/$R_5SO_3^-$ did not show the surface-wave behavior. Figure 4 shows the relationship between the X-value and the carbon number of the dopant (n). The X-value was estimated to be in the range 200—500 mV s^{-1}. The X-value decreased with the dopant size at $n<5$, and gradually increased with the dopant size at $n>6$. The X-value reflects the mobility of ionic species in the PPy matrix. In other words, when X=1, the mobility of ionic species is high, but when X=0.5, that of ionic species is low. Accordingly, it was concluded that the mobilities of the ionic species in PPy/$R_3SO_3^-$ and PPy/$R_{10}SO_3^-$ were high, and that in PPy/$R_5SO_3^-$ was low. Assuming only the anion can be transported in the PPy matrix, the mobility of $R_{10}SO_3^-$ was higher than that of $R_5SO_3^-$. Thus, the present observation can not be explained only by the dopant size. It was considered that other ionic species, an electrolyte cation, contributed to the electrochemical doping-undoping process. We had already reported that in the case that the polymer anion incorporated PPy (PPy/PA), the electrolyte cation was incorporated into the PPy matrix in lieu of the anion, when the PPy was electrochemically reduced.[32]

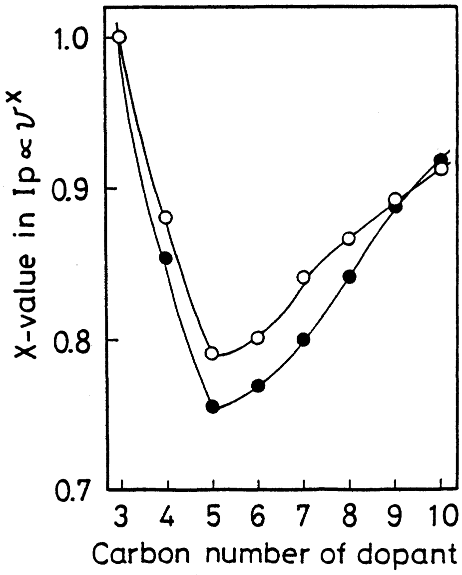

Fig. 4. Relationship between X and carbon number of dopant for PPy/$R_nSO_3^-$. X-Values were estimated from the slope between $\log(i_p)$ and $\log(v)$ (v were in the range 200—500 mV s^{-1}).

Cyclic voltammetry for PPy/$R_nSO_3^-$ in H_2O containing KCl was carried out in order to estimate only the mobility of the anion. Figure 5 shows typical cyclic vltammograms of PPy/$R_nSO_3^-$ (n=3, 5, and 10) in H_2O containing 0.1 mol dm^{-3} KCl as a supporting electrolyte. We have already reported that the PPy/Cl^- had a more positive redox potential (>0 V vs. SCE) than the PPy/$R_5SO_3^-$, and that the potential sweeps in cyclic voltammetry for PPy/$R_5SO_3^-$ in a KCl aqueous solution induced an exchange reaction of the dopants (PPy/$R_5SO_3^-$ → PPy/Cl^-).[33] The rate of dopant exchange is controlled by the mobility of the original dopant in the PPy matrix, so that the diffusion rate of the original dopant can be estimated by the rate of the dopant-exchange reaction. Changes of the cyclic voltammograms during 5 sweeps can be observed in Fig. 5. The redox peaks at low and high potentials corresponded to the oxidation-reduction of PPy/$R_nSO_3^-$ and PPy/Cl^-, respectively. The redox peaks of PPy/$R_nSO_3^-$ decreased and those of PPy/Cl^- increased in all cyclic voltammograms. The cyclic voltammograms for PPy/$R_3SO_3^-$ and PPy/$R_5SO_3^-$ were profoundly changed. On the contrary, the cyclic voltammogram for PPy/$R_{10}SO_3^-$ was hardly changed. The rate of change of the peak currents decreased with the dopant size. Upon the first reduction of PPy, the original dopant, $R_nSO_3^-$, was partly released from the PPy matrix. On the successive oxidation, Cl^- in the electrolytic solution was partly incorporated into the PPy, since the concentration of Cl^- in the electrolytic solution was much higher than that of $R_nSO_3^-$. We defined a convenient dopant exchange rate as

$$\Phi = 1 + (i_{pc}(Cl^-)/i_{pc}(R_nSO_3^-)) \text{ at 5th cycle,} \qquad (1)$$

Φ increased with the mobility of $R_nSO_3^-$. Figure 6 shows the relationship between Φ and the carbon number of the dopant. Φ decreased with the dopant size, which indicates that the mobility of the $R_nSO_3^-$ decreased with the dopant size. This conclusion could not explain the profile of Fig. 4, in which the mobility of the ionic species does not monotonously decrease with the dopant size. The increasing mobility observed for the longer alkyl dopants (n=5—10) in Fig. 4 should be explained by the incorporation of an electrolyte cation into the PPy matrix. We already reported that the electrolyte cation, e.g., K^+, was incorporated into the PPy matrix in order to conserve the electro-neutrality in the PPy matrix when the PPy/PA was electrochemically reduced. In this case, the polymer anion dopant was not released from the PPy matrix, owing to its macromolecularity. We called this observation "a pseudo-cathodic doping" and the polymer anion dopant "an immobilized dopant." It was suggested that the long alkyl dopants, such as $R_{10}SO_3^-$, were partly immobilized in the PPy matrix as a polymer anion dopant, so that the electrolyte cation was partly incorporated and released upon the oxidation and reduction of PPy. Because K^+ is much smaller than $R_nSO_3^-$, the increasing mobility observed for longer alkyl dopants in Fig. 4 could be explained by the incorporation of K^+ instead of the release of $R_nSO_3^-$.

Cation-Exchange Capability of PPy/$R_nSO_3^-$. We have reported that a novel type of electrochemical deionization system was constructed using a PPy/Cl^- (red.) anode and a PPy/PA cathode.[39,40] In this system an electrolyte anion was incorporated into the PPy/Cl^- by ordinary doping and an electrolytic cation was incorporated into PPy/PA by pseudo-cathodic doping. Thus, the PPy/Cl^- had an anion-exchange ability, and the PPy/PA had a cation-exchange ability. Electrochemical deionization experiments were carried out using an PPy/Cl^- (red.) anode and the present PPy/$R_nSO_3^-$ cathode in order to reveal a cation-

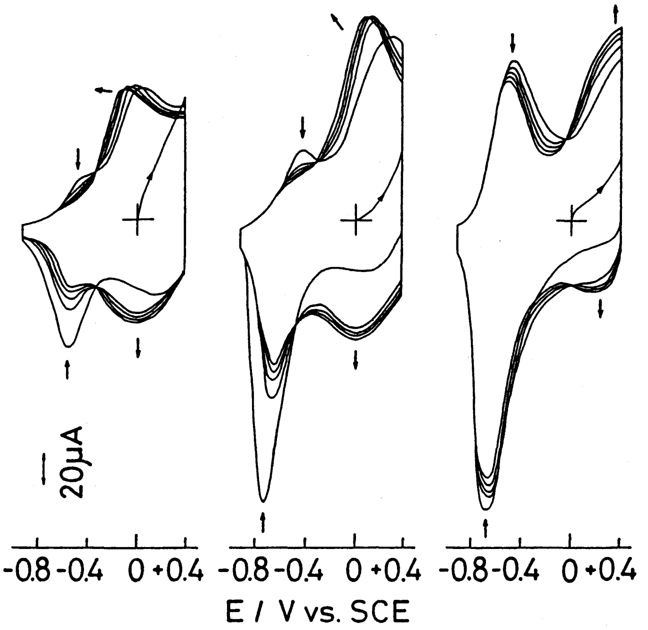

Fig. 5. Cyclic voltammograms of PPy/$R_3SO_3^-$ (left), PPy/$R_5SO_3^-$ (middle), and PPy/$R_{10}SO_3^-$ (right) in H_2O containing KCl (0.1 mol dm^{-3}) under potential sweep. Sweep rate was 200 mV s^{-1}.

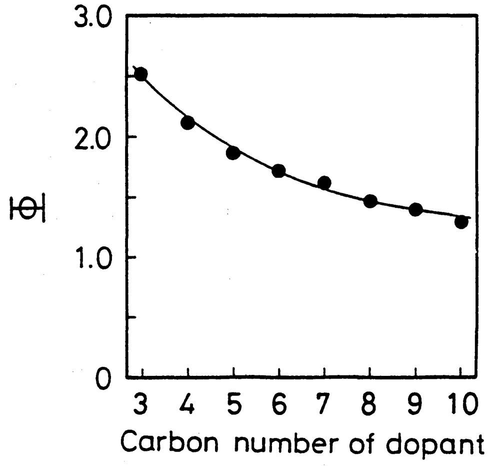

Fig. 6. Relationship between Φ and carbon number of dopant. Φ is defined by Eq. 1.

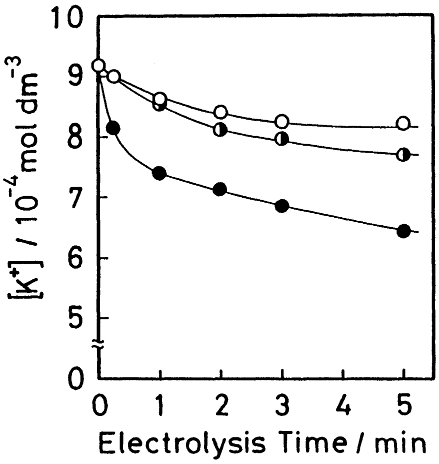

Fig. 7. Change of K^+ concentration in KCl aqueous solution with deionization time on 4 V potentiostatic electrolysis, using a PPy/Cl^- (red.) anode and a PPy/$R_nSO_3^-$ cathode. (○); PPy/$R_3SO_3^-$, (◑); PPy/$R_5SO_3^-$, and (●); PPy/$R_{10}SO_3^-$.

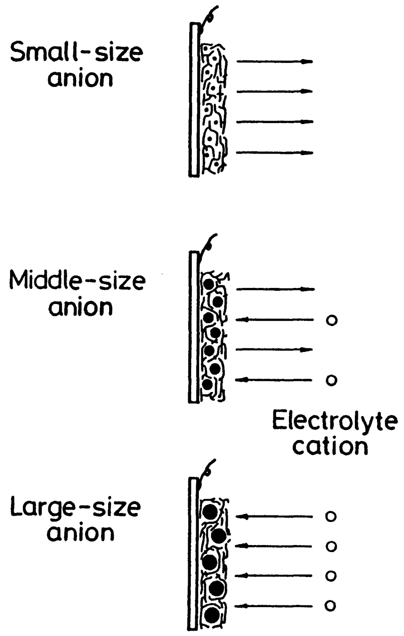

Fig. 8. A proposed model for the doping-undoping behavior of PPy/$R_nSO_3^-$.

exchange capability, i.e., the pseudo-cathodic doping, of the PPy/$R_nSO_3^-$. In these experiments the PPy/Cl^- (red.) was used as an anode in order to prevent any pH change in the solution and to promote the effective deionization of K^+.40) Figure 7 shows the concentration change of K^+ in a KCl aqueous solution (original; 9.2×10^{-4} mol dm^{-3}) treated by the potentiostatic electrolysis (4 V) of the two electrodes. The concentration of K^+ decreased as a result of this treatment. The quantity of incorporated K^+ increased with the dopant size. This observation indicated that PPy/$R_nSO_3^-$ had a considerable capability of pseudo-cathodic doping. Moreover, the capability of pseudo-cathodic doping increased with the dopant size.

Figure 8 shows a proposed model for the doping-undoping behavior of PPy/$R_nSO_3^-$. Controlling such a dual-mode behavior, the release of an anion or the incorporation of a cation, of the present films will provide a prismatic electerochemical material.

This work was partly supported by a Grant-in-Aid from the Ministry of Education.

References

1) A. F. Diaz, K. K. Kanazawa, and G. P. Gardini, *J. Chem. Soc., Chem. Commun.*, **1979**, 635.

2) K. K. Kanazawa, A. F. Diaz, R. H. Geiss, W. D. Gill, J. F. Kwak, J. A. Logan, J. F. Rabolt, and G. B. Street, *J. Chem. Soc., Chem. Commun.*, **1979**, 854.

3) A. F. Diaz and J. I. Castillo, *J. Chem. Soc., Chem. Commun.*, **1980**, 397.

4) A. F. Diaz, J. I. Castillo, J. A. Logan, and W.-Y. Lee, *J. Electroanal. Chem.*, **129**, 115 (1981).

5) A. F. Diaz, A. Martinez, K. K. Kanazawa, and M. Salmon, *J. Electroanal. Chem.*, **130**, 181 (1981).

6) A. F. Diaz, J. I. Castillo, K. K. Kanazawa, J. A. Logan, M. Salmon, and O. Fajardo, *J. Electroanal. Chem.*, **133**, 233 (1981).

7) H. S. White, G. P. Kittlesen, and M. S. Wrighton, *J. Am. Chem. Soc.*, **106**, 5375 (1984).

8) G. P. Kittlesen, H. S. White, and M. S. Wrighton, *J. Am. Chem. Soc.*, **106**, 7389 (1984).

9) F. Garnier, G. Tourillon, M. Gazard, and J. C. Dubois, *J. Electroanal. Chem.*, **148**, 299 (1983).

10) R. Bjorklund, S. Andersson, S. Allenmark, and I. Lundström., *Mol. Cryst. Liq. Cryst.*, **121**, 263 (1985).

11) S. Kuwabata, H. Yoneyama, and H. Tamura, *Bull. Chem. Soc. Jpn.*, **57**, 2247 (1984).

12) K. Kaneto and Y. Yoshino, *Kino Zairyo (Jpn.)*, **4**, 8 (1984).

13) A. Mohammadi, O. Inganas, and I. Lundström, *J. Electrochem. Soc.*, **133**, 947 (1986).

14) N. Mermilliod, J. Tanguy, and F. Petiot, *J. Electrochem. Soc.*, **133**, 1073 (1986).

15) T. Osaka, K. Naoi, H. Sasaki, and S. Ogano, *J. Electrochem. Soc.*, **134**, 285 (1987).

16) A. F. Diaz, *Chemica Scripta.*, **17**, 145 (1981).

17) P. Burgmayer and R. W. Murray, *J. Am. Chem. Soc.*, **104**, 6139 (1982).

18) P. Burgmayer and R. W. Murray, *J. Phys. Chem.*, **88**, 2515 (1984).

19) A. F. Diaz, W.-Y. Lee, A. Logan, and D. C. Green, *J. Electroanal. Chem.*, **108**, 377 (1980).

20) R. A. Bull, F.-R. Fan, and A. J. Bard, *J. Electrochem. Soc.*, **130**, 1636 (1983).

21) R. Noufi, *J. Electrochem. Soc.*, **130**, 2126 (1983).

22) K. Okabayashi, O. Ikeda, and H. Tamura, *J. Chem. Soc., Chem. Commun.*, **1983**, 684.

23) R. B. Bjorklund and I. Lundström, *J. Electron. Mater.*, **13**, 211 (1984).

24) O. Niwa and T. Tamamura, *J. Chem. Soc., Chem. Commun.*, **1984**, 817.

25) S. E. Lindsey and G. B. Street, *Synth. Metals*, **10**, 67 (1984).

26) M-A. de Paoli, R. J. Waltman, A. F. Diaz, and J. Bargon, *J. Chem. Soc., Chem. Commun.*, **1984**, 1015.

27) N. Bates, M. Cross, R. Lines, and D. Walton, *J. Chem. Soc., Chem. Commun.*, **1985**, 871.

28) T. Ojio and S. Miyata, *Polym. J.*, **18**, 95 (1986).

29) F.-R. F. Fan and A. J. Bard, *J. Electrochem. Soc.*, **133**, 301 (1986).

30) H. Yoneyama, T. Hirai, S. Kuwabata, and O. Ikeda, *Chem. Lett.*, **1986**, 1243.

31) T. Iyoda, A. Ohtani, T. Shimidzu, and K. Honda, *Synth. Metals*, **18**, 725 (1987).

32) T. Iyoda, A. Ohtani, T. Shimidzu, and K. Honda, *Chem. Lett.*, **1986**, 687.

33) T. Shimidzu, A. Ohtani, T. Iyoda, and K. Honda, *J. Electroanal. Chem.*, **224**, 123 (1987).

34) J. H. Kaufmann, K. K. Kanazawa, and G. B. Street, *Phys. Rev. Lett.*, **53**, 2461 (1984).

35) E. M. Genies and J. M. Pernaut, *Synth. Metals*, **10**, 117 (1984).

36) G. Nagasubramanian, S. Di Stefano, and J. Moacanin, *J. Phys. Chem.*, **90**, 4447 (1986).

37) W. Wernet, M. Monkenbusch, and G. Wegner, *Makromol. Chem., Rapid Commun.*, **5**, 157 (1984).

38) N. Oyama and F. C. Anson, *J. Electrochem. Soc.*, **127**, 640 (1980).

39) T. Shimidzu, A. Ohtani, T. Iyoda, and K. Honda, *J. Chem. Soc., Chem. Commun.*, **1986**, 1415.

40) T. Shimidzu, A. Ohtani, and K. Honda, *J. Electroanal. Chem.*, in press.